

## NUMERICAL STUDY ON NATURAL CONVECTION OF MWCNT NANOFUIDS IN A ENCLOSURE BASED ON EXPERIMENTAL CONDUCTIVITY AND VISCOSITY

I.D. Garbadeen, M. Sharifpur\*, J. Slabber and J.P. Meyer  
Department of Mechanical and Aeronautical Engineering,  
University of Pretoria, Pretoria, 0002, South Africa,

\*Author for correspondence

[mohsen.sharifpur@up.ac.za](mailto:mohsen.sharifpur@up.ac.za)

Keywords: Nanofluids, Natural Convection, MWCNT, Nusselt Number, Thermal Conductivity, Viscosity

### ABSTRACT

This study is motivated by the much reported enhancement in thermal conductivity of nanofluids and their potential as a replacement for conventional coolant fluids. Among the various factors considered in the selection of a coolant fluid, this study focused on the convective behaviour of nanofluids as demonstrated in a square enclosure with differentially heated side walls at low particle concentrations of 0 – 1 % and Ra number range of  $10^4$  to  $10^6$ . Therefore, the study consists of numerical investigation by using experimentally determined thermal conductivities and viscosities of the nanofluid. A theoretical model was used for higher (though less practical) particle concentration of up to 8 %. The simulations were done by using CD Adapco's Star-CCM+ Code (v 8.06) revealed an initial enhancement in the Nusselt number with varying particle concentration before rapidly falling to an average value that continues to diminish for the concentration range tested. This was true for different Ra numbers. The variation was attributed to the counteracting, non-linear effects of thermal conductivity and viscosity both of which increases by increasing particle concentration. The thermal conductivity effect were observed to be more dominant for a very narrow range of low particle concentration below 0.1 % while the viscous effect was found to be the more dominant at higher particle concentration above 0.1 %.

### NOMENCLATURE

$c_p$	Specific heat capacity
$d$	Particle diameter
DI	De-ionised Water
$g$	Acceleration due to gravity
$k$	Thermal conductivity
$k_{eff}$	Effective thermal conductivity
$L$	Length
$Nu$	Nusselt number
$Pr$	Prandtl number

$q$	Rate of heat transfer
$r$	Radius
$Ra$	Rayleigh number
$Re$	Reynolds number
$T$	Temperature
$v_s$	sedimentation velocity
$\mu$	Dynamic viscosity
$\alpha$	Diffusivity; temperature coefficient of resistance
$\beta$	Thermal coefficient
$\rho$	Base fluid density; resistivity coefficient
$\phi$	Volume concentration of particles

### INTRODUCTION

Natural convection continues to be an area of interest in research because of its potential use in a myriad of applications including computer cooling, aeronautics, automobiles, nuclear power plants, solar energy, aeolian and geothermal equipment, as well as the food, agriculture and pharmaceutical industry [1]. However, there appears to be a greater focus on thermal conductivity than convection despite the fact that it is improved heat transfer in convective conditions that gives a sufficient motivation for usage of nanofluids and not simply enhancement in thermal conductivity [2]. Nevertheless, nanofluids as a new heat transfer fluid still hasn't made a significant breakthrough in heat transfer applications to date.

Ternik and Rudolf [3] numerically investigated natural convection of Au,  $Al_2O_3$ , Cu and  $TiO_2$  aqueous nanofluids in the range  $10^3 \leq Ra \leq 10^5$  using 0 – 10% volume concentration ( $\phi$ ). For each type of nanofluid they investigated, the average Nusselt number along with overall heat transfer enhancement increased with both Rayleigh number and volume concentration. Greater enhancement was found for lower Rayleigh numbers. Enhancement values as high as 33% for  $Ra = 10^5$  and  $\phi = 0.1$ . These findings were supported by Khanafer's *et al.* [4] numerical analysis using aqueous copper nanofluids in a two-dimensional enclosure and Grashof number ranging from

$10^3 - 10^5$ . The nanofluid was treated as single-phase with different thermal conductivity and viscosity models applied. An increase in heat transfer rate was found at each Grashof number. Nusselt number was also found to increase with volume concentration for the range  $0 \leq \phi \leq 0.1$  and Rayleigh number  $10^4 \leq Ra \leq 10^5$ . A similar study to Khanafer *et al* [4] was done by Santra *et al.* [5] where natural convection of aqueous copper nanofluids in a square enclosure over  $10^4 \leq Ra \leq 10^7$  and  $0.05\% \leq \phi \leq 5\%$ . Interestingly a decrease in heat transfer was observed over any given Ra number with increasing volume concentration. A decrease in average Nusselt number was as high as 38.3% for  $\phi = 5\%$  and  $Ra = 10^7$ . Furthermore, Santra *et al.* observed the average Nusselt number was independent on the volume concentration,  $\phi > 3\%$  at  $Ra = 10^4$ . This particular result was corroborated by Abu-Nada [6] who used horizontal concentric annuli instead of a square enclosure. They reported heat transfer enhancement for  $Ra = 10^3$  and  $Ra = 10^5$  but intermediate values showed a reduction in heat transfer with negligible effect of volume concentration on heat transfer at  $Ra = 10^4$ . The studies above have the limitation of using idealised models for thermal conductivity and viscosity which often differ significantly with actual nanofluid behaviour. There is a wide range of possible models to select from and Ho *et al.* [7] demonstrated that the choice of model significantly affects and sometimes lead to contradictory results. This finding is supported by the disparity in Khanafer *et al.* [4] and Santra *et al.* [5] results.

More recently, the discrepancies in natural convection studies of nanofluid was extended by Jahanshahi *et al.* [8] who observed an increase in average Nusselt number with increasing particle concentration for Rayleigh number  $10^3 - 10^5$  and particle volume fraction  $0 - 4\%$ . The thermal conductivity values used were obtained experimentally instead of relying on theoretical models. Similarly, the numerical analysis in the present study is also supplemented by experimental characterisation of the thermo-physical properties of the MWCT. To the author's best knowledge, no study on natural convection in carbon nanofluids is reported. This paper therefore focuses on natural convection of MWCNT in a square enclosure and forms part of an on-going numerical and experimental study of natural convection in nanofluids.

## ANALYSIS AND MODELLING

A 2D square enclosure is considered with length  $L$  and differential heated side walls of temperature

$T_H$  and  $T_L$ . Top and bottom walls are considered to be well insulated and therefore adiabatic.

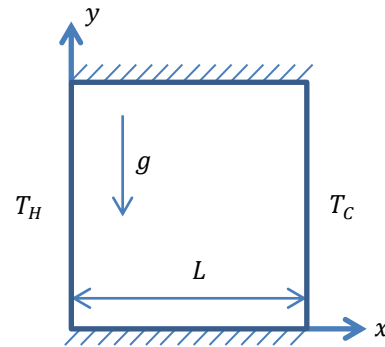


**Figure 1:** Physical Model for Problem and Coordinate System

The nanofluid is treated as single-phase homogeneous, Newtonian and incompressible and the flow generated is laminar. Furthermore, viscous heat dissipation in the energy equation is considered negligible. The hydrodynamic and thermal fields are related using Boussinesq's approximation which requires density of the fluid to vary. The averages of the other thermo-physical properties are assumed constant in the enclosure and are given in Table 1.

**Table 1:** Thermo-physical properties of base fluid and nanoparticle

Property	Water	MWCT
$\rho$ ( $kg/m^3$ )	997.1	2100
$k$ ( $W/mK$ )	0.613	15
$c_p$ ( $J/KgK$ )	4179	470
$\beta$ ( $1/K$ )	0.00021	0.000007

The nanofluid samples prepared using the two-step method by ultrasonication. After preparation, the nanofluid thermal conductivity data was measured by using a handled Decagon KD2 Pro thermal properties analyser with  $\pm 5\%$  error. The SV10 Sine-wave Vibro Viscometer with  $\pm 1\%$  error was used in measuring viscosity. All nanofluid samples maintained stability beyond experimentation time.

With the preceding considerations and assumptions, applying Navier Stokes equations to the model gives the following equations:

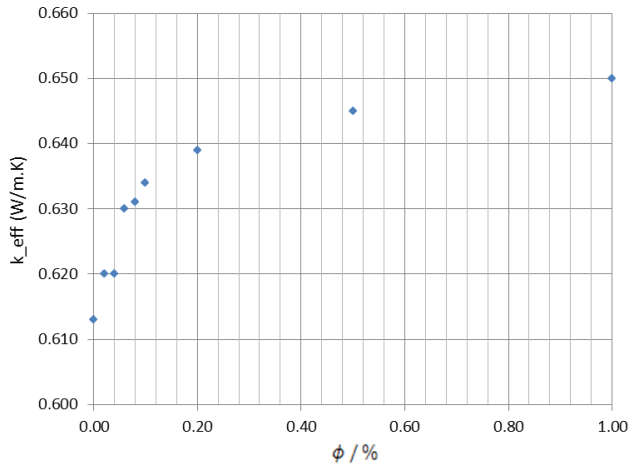


**Figure 2:** Experimental values of thermal conductivity at varying  $\phi$

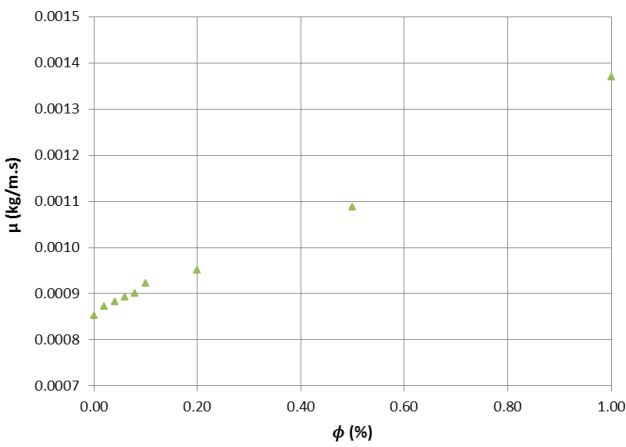


**Figure 3:** Experimental values of viscosity at varying  $\phi$  at 300K

Continuity:

$$\nabla \cdot \mathbf{v} = 0$$

Momentum:

$$\rho \frac{D\mathbf{V}}{Dt} = -\nabla P + \nabla \cdot (\mu \nabla \mathbf{u}) + (\rho\beta)_n \mathbf{g} (T - T_c)$$

Energy:

$$\frac{DT}{Dt} = \nabla \cdot \left( \frac{k}{(\rho c_p)_n} \nabla T \right)$$

The thermo-physical properties used in the above equations vary with volume concentration as follows:

Density:

$$\rho_n = (1 - \phi)\rho_f + \phi\rho_s$$

Specific Heat:

$$(\rho c_p)_n = (1 - \phi)(\rho c_p)_f + \phi(\rho c_p)_s$$

Thermal expansion coefficient:

$$(\rho\beta)_n = (1 - \phi)(\rho\beta)_f + \phi(\rho\beta)_s$$

Buoyancy source term

$$\mathbf{f}_g = \rho \mathbf{g} \beta (T_{ref} - T)$$

with  $T_{ref}$  as the bulk temperature of the nanofluid

The following boundary conditions follow from the formulation above:

Adiabatic top and bottom wall:

$$\frac{\partial T}{\partial y} = 0 \quad 0 \leq x \leq L \text{ and } y = 0, H$$

Constant temperature sidewall:

$$T = T_H; \quad T = T_C; \quad x = 0; \quad x = L;$$

No-slip boundary condition:

$$u = v = 0$$

$$x = 0 \text{ and } 0 \leq y \leq L$$

$$x = L \text{ and } 0 \leq y \leq L$$

$$y = 0 \text{ and } 0 \leq x \leq L$$

$$y = L \text{ and } 0 \leq x \leq L$$

### Mesh Independence Study and Validation

Both mesh generation and simulation was done using CD Adapco's Star-CCM+ Code (v 8.06). Since the domain of analysis is relatively simple, the need for compromise between computational cost and fidelity of results that one usually encounters when performing CFD calculations is not present. Mesh refinement was carried out until there was no significant change in Nusselt number obtained. At this point the solution can be considered to be independent of the meshing applied to the domain.

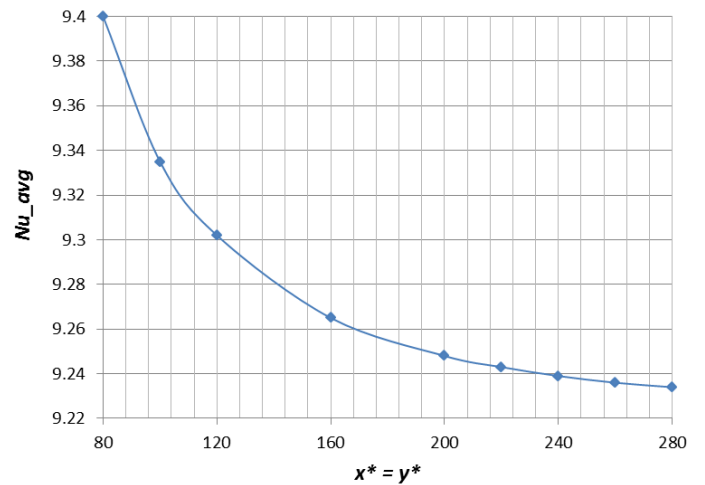


**Figure 4:** Convergence of  $Nu_{avg}$  with increasing mesh refinement ( $x^* = y^*$ )

From the various meshing types available, a square grid was applied to a 2D model. Results for maximum and average Nusselt number, along the hot wall for water filled square cavity at  $Ra = 10^6$  are given in Figure 2. Nusselt number was calculated as:

$$Nu_H = -\frac{k_n}{k_f} \frac{\partial T(y)}{\partial x} \Big|_{x=0}$$

The mesh size  $x^* = y^* = 280$  was obtained. To validate the simulation parameter, Numerical analysis was done for an air-filled square enclosure at  $Ra$  number  $10^4 - 10^6$  and  $Pr = 0.71$ .

Results were compared with previous works of De Vahl [9] and Turan and Poole [10] which indicated in Table 2. The maximum deviation of 1.6 % was calculated which occurs at  $Ra = 10^6$  between the current study and De Vahl.

**Table 2:** Comparison between current and previous works

$Ra$		Current Study	(De Vahl Davis, 1983)	(Turan et al. 2010)
$10^3$	$Nu_{avg}$	1.118	1.118	1.118
	$Nu_{max}$	1.502	1.506	1.506
$10^4$	$Nu_{avg}$	2.252	2.243	2.245
	$Nu_{max}$	3.539	3.528	3.531
$10^5$	$Nu_{avg}$	4.519	4.519	4.520
	$Nu_{max}$	7.725	7.717	7.717
$10^6$	$Nu_{avg}$	8.830	8.799	8.823
	$Nu_{max}$	17.650	17.925	17.530

## RESULTS AND DISCUSSION

The temperature distribution is taken at the mid-plane of the cavity with normal vector  $[x, y, z] = [0, 0, 1]$  for non-dimensionalised temperature  $T^* = (T - T_c)/(T_h - T_c)$  and shown in figures 5 – 7. There exists a region around the core of the cavity where temperature is uniform and at approximately the average of the two wall temperatures of 300 K. It can be seen that as the  $Ra$  increases, the region increases in size. Another view is that for a given  $\phi$ , increasing  $Ra$  corresponds with increasing non-linearity of the temperature profiles. This is due the increased buoyancy effect while viscous forces remain fairly constant, in turn increasing the strength of the convective currents. However, for the particle concentration range under consideration, there is *no* significant effect when changing  $\phi$  on the temperature profiles.

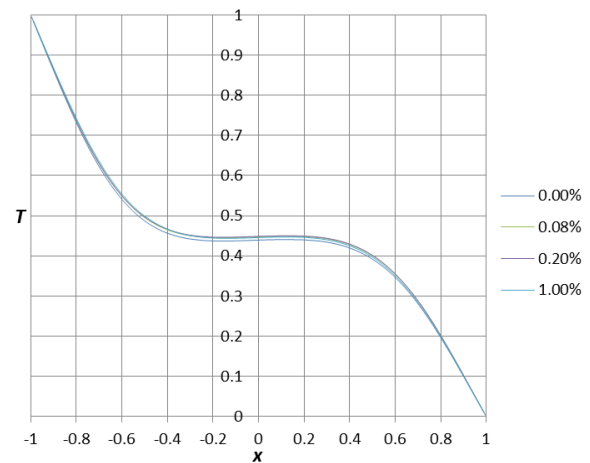


**Figure 5:** Temperature variation along axial midline  $x = [-1, 1]$  for different volume concentration ( $\phi$ ) at  $Ra = 10^4$

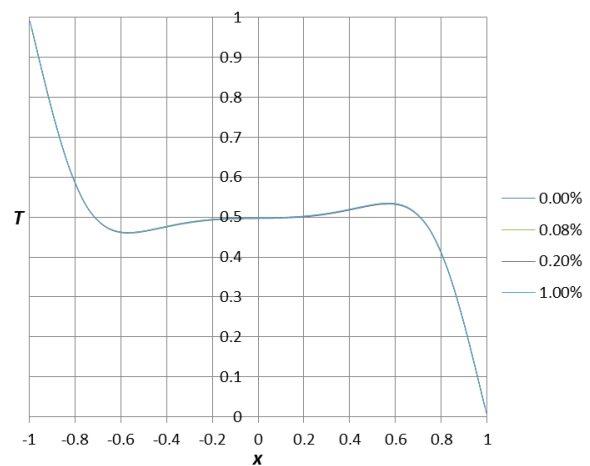


**Figure 6:** Temperature variation along axial midline  $x = [-1, 1]$  for different volume concentration ( $\phi$ ) at  $Ra = 10^5$

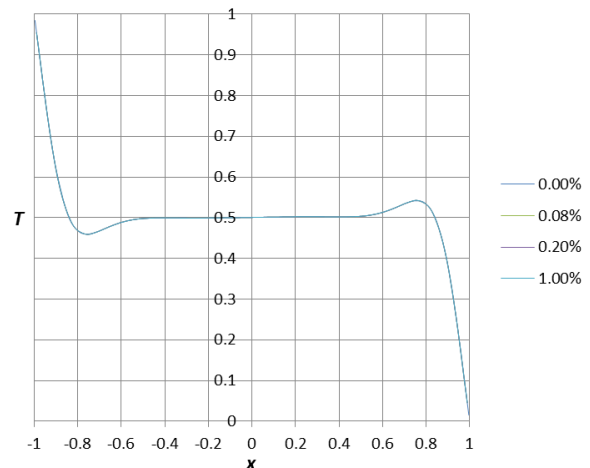


**Figure 7:** Temperature variation along axial midline  $x = [-1, 1]$  for different volume concentration ( $\phi$ ) at  $Ra = 10^6$

This can be attributed to the increases in thermal conductivity and viscosity, both of which have antagonistic effects on convective heat transfer, being equally matched which illustrates

the core of the present study. The change in buoyancy forces and the viscous forces are virtually cancelled out as  $\phi$  increases therefore registering any significant change in the temperature profile.

The velocity distribution in the y-direction is taken at the mid-plane with normal vector  $[x, y, z] = [0, 1, 0]$ .

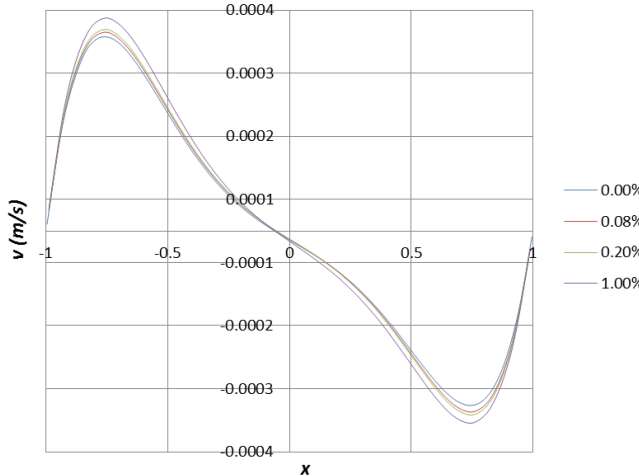


**Figure 8:** Y-velocity variation along axial midline  $x = [-1, 1]$  for different volume concentration ( $\phi$ ) at  $Ra = 10^4$

From figures 8 to 10, the maximum velocity at each value of  $Ra$  increases with increasing  $\phi$ . Similarly to the temperature profiles, the size of the central region with uniform velocity increases with  $Ra$  number. Also the absolute maximum velocity increases with  $Ra$  number. This is attributed to the increased buoyancy effect. For a given  $\phi$  value, increasing  $Ra$  strengthens the buoyancy effects while viscous effects remain fairly constant thereby increasing the overall convective heat transfer. However, for the range considered, variation with  $\phi$  is minimal and this due to the same effect explained for the temperature profiles.

Thermal conductivity and viscosity have a counteracting effect on convective heat transfer and the central problem that arises is which of the two properties is dominant? Increase in maximum velocity with  $\phi$  values indicates the increase in thermal conductivity (which strengthens the buoyancy effect) out slightly outbalances the increase in viscosity which tends to decrease the overall buoyancy effect. Although increasing  $\phi$  is expected to cause the fluid to become more viscous and reduce the velocities, the increase in thermal conductivity counters this effect by increasing convection. There's increased penetration of heat in the fluid with increasing  $\phi$  therefore the central region of uniform velocity decreases with increasing  $\phi$ .

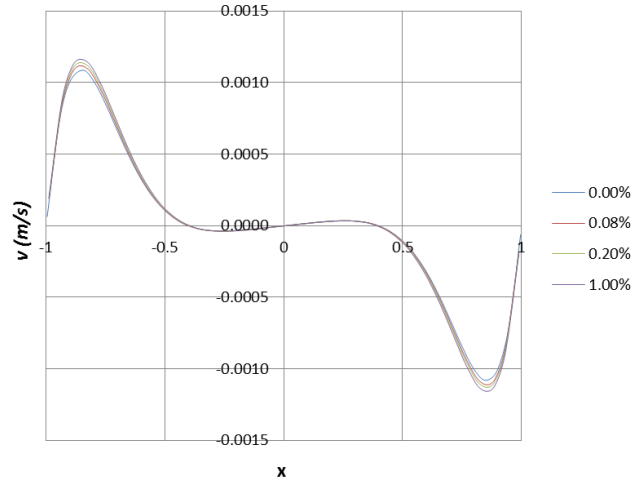


**Figure 9:** Y-velocity variation along axial midline  $x = [-1, 1]$  for different volume concentration ( $\phi$ ) at  $Ra = 10^5$

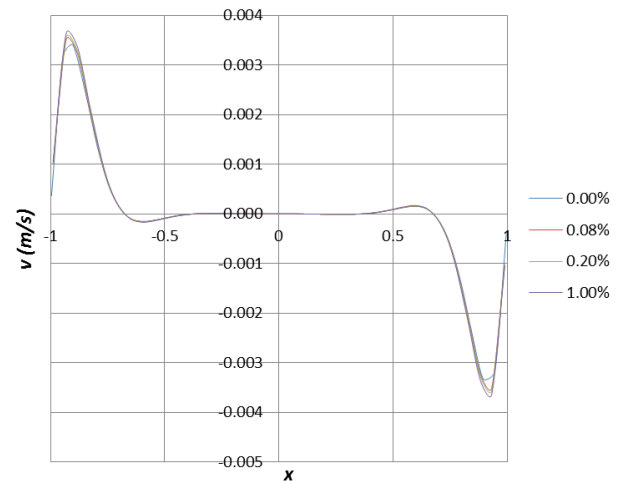


**Figure 10:** Y-velocity variation along axial midline  $x = [-1, 1]$  for different volume concentration ( $\phi$ ) at  $Ra = 10^6$

In Figure 11 Nusselt number at low concentration below 0.1 %, reaches maxima besides which Nusselt number declines rapidly to an average value. The ratio of Nusselt number maxima to the reference ( $Nu_{\phi=0}$ ) increases with increasing  $Ra$  number. This could be explained by the relatively low viscosity at low particle concentration while the thermal conductivity effect dominates resulting in an overall enhancement in heat transfer. Between 0.2 and 1.0 % the change in Nusselt number is minimal although a gradual decrease can be observed especially for higher Rayleigh numbers. This indicates that for this range of  $\phi$  values, the desirable effects of high thermal conductivity and the undesirable effects of increased viscosity combine to have an overall minimal influence on the Nusselt number. This was reported by Ternik and Rudolf [11] who found the same trend for nanofluids of Au,  $Al_2O_3$ , Cu and

TiO<sub>2</sub> for  $10^3 \leq Ra \leq 10^5$  using 0 – 10% volume concentration ( $\phi$ ).

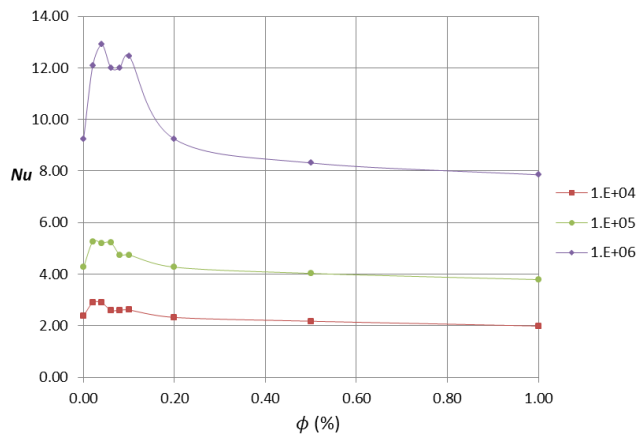


**Figure 11:** Variation of average Nusselt number on the hot wall with volume concentration ( $\phi$ ) at different Rayleigh number

## CONCLUSIONS

The heat transfer performance of MWCNT nanofluids in a square enclosure has been studied for the range of particle volume concentrations  $0 \leq \phi \leq 1.0\%$  using experimentally determined values of thermal conductivity and viscosity. The heat transfer performance was calculated for Rayleigh number of  $10^4 - 10^6$  with base fluid at Prandtl number 5.83. CD Adapco's Star-CCM+ Code (v 8.06) was used to carry out the numerical study. From the analysis of heat transfer in a square enclosure filled with nanofluids of varying particle concentration, there was an increase in heat transfer performance as characterized by the Nusselt number with increasing Ra number. Between  $Ra = 10^4$  and  $Ra = 10^6$ , there was a 130% increase in the average Nusselt number. This was corroborated by previous results available in the literature. The combined effect of both increasing thermal conductivity and increasing viscosity due to increasing particle concentration had an enhancement effect on the heat transfer performance below 0.1 %.

## REFERENCES

[1] A. Baïri, E. Zarco-Pernia, and J. M. García De María, "A review on natural convection in enclosures for engineering applications. the particular case of the parallelogrammic diode cavity," *Applied Thermal Engineering*, vol. 63, no. 1, pp. 304–322, 2014.

[2] S. K. Das, S. U. S. Choi, and H. E. Patel, "Heat Transfer in Nanofluids — A Review Heat Transfer in Nanofluids —," no. January 2013, pp. 37–41, 2007.

[3] P. Ternik and R. Rudolf, "Heat transfer enhancement for natural convection flow of water-based nanofluids in a square enclosure," *International Journal of Simulation Modelling*, vol. 11, no. 1, pp. 29–39, Mar. 2012

[4] K. Khanafer, K. Vafai, and M. Lightstone, "Buoyancy-driven heat transfer enhancement in a two-dimensional enclosure utilizing nanofluids," *International Journal of Heat and Mass Transfer*, vol. 46, no. 19, pp. 3639–3653, Sep. 2003.

[5] A. K. Santra, S. Sen, and N. Chakraborty, "Study of heat transfer augmentation in a differentially heated square cavity using copper–water nanofluid," *International Journal of Thermal Sciences*, vol. 47, no. 9, pp. 1113–1122, Sep. 2008.

[6] E. Abu-Nada, Z. Masoud, and a. Hijazi, "Natural convection heat transfer enhancement in horizontal concentric annuli using nanofluids," *International Communications in Heat and Mass Transfer*, vol. 35, no. 5, pp. 657–665, May 2008.

[7] C. J. Ho, M. W. Chen, and Z. W. Li, "Numerical simulation of natural convection of nanofluid in a square enclosure: Effects due to uncertainties of viscosity and thermal conductivity," *International Journal of Heat and Mass Transfer*, vol. 51, no. 17–18, pp. 4506–4516, Aug. 2008.

[8] M. Jahanshahi, S. F. Hosseinizadeh, M. Alipanah, a. Dehghani, and G. R. Vakilnejad, "Numerical simulation of free convection based on experimental measured conductivity in a square cavity using Water/SiO<sub>2</sub> nanofluid," *International Communications in Heat and Mass Transfer*, vol. 37, no. 6, pp. 687–694, Jul. 2010.

[9] G. De Vahl Davis, "Natural convection of air in a square cavity: a bench mark numerical solution," *International Journal for Numerical Methods in Fluid*, vol. 3, pp. 249–264, 1983.

[10] O. Turan, N. Chakraborty, and R. J. Poole, "Laminar natural convection of Bingham fluids in a square enclosure with differentially heated side walls," *Journal of Non-Newtonian Fluid Mechanics*, vol. 165, no. 15–16, pp. 901–913, Aug. 2010.

[11] P. Ternik and R. Rudolf, "Laminar Natural Convection of Non-Newtonian Nanofluids in a Square Enclosure with Differentially Heated Side Walls," *International Journal of Simulation Modelling*, vol. 12, no. 1, pp. 5–16, Mar. 2013